Thick escaping magnetospheric ion layer in magnetopause reconnection with MMS observations

T. Nagai, N. Kitamura, H. Hasegawa, I. Shinohara, S. Yokota, Y. Saito, R. Nakamura, B. L. Giles, C. Pollock, T. E. Moore, et al.

AGU PUBLICATIONS

Geophysical Research Letters

RESEARCH LETTER
10.1002/2016GL069085

Special Section:
First results from NASA's Magnetospheric Multiscale (MMS) Mission

Thick escaping magnetospheric ion layer in magnetopause reconnection with MMS observations

T. Nagai[1], N. Kitamura[2], H. Hasegawa[2], I. Shinohara[2], S. Yokota[2], Y. Saito[2], R. Nakamura[3], B. L. Giles[4], C. Pollock[4,5], T. E. Moore[4], J. C. Dorelli[4], D. J. Gershman[4,6], W. R. Paterson[4], L. A. Avanov[4,6], M. O. Chandler[7], V. Coffey[7], J. A. Sauvaud[8,9], B. Lavraud[8,9], C. T. Russell[10], R. J. Strangeway[10], M. Oka[11], K. J. Genestreti[12,13], and J. L. Burch[13]

[1]Department of Earth and Planetary Sciences, Tokyo Institute of Technology, Tokyo, Japan, [2]Institute of Space and Astronautical Science, Japan Aerospace Exploration Agency, Sagamihara, Japan, [3]Space Research Institute, Austrian Academy of Sciences, Graz, Austria, [4]NASA Goddard Space Flight Center, Greenbelt, Maryland, USA, [5]Now at Denali Scientific, Healy, Alaska, USA, [6]Department of Astronomy, University of Maryland, College Park, Maryland, USA, [7]NASA Marshall Space Flight Center, Huntsville, Alabama, USA, [8]Institut de Recherche en Astrophysique et Planétologie, Université de Toulouse, Toulouse, France, [9]Centre National de la Recherche Scientifique, UMR 5277, Toulouse, France, [10]Department of Earth, Planetary, and Space Sciences, University of California, Los Angeles, California, USA, [11]Space Science Laboratory, Berkeley, California, USA, [12]Department of Physics and Astronomy, University of Texas at San Antonio, San Antonio, Texas, USA, [13]Southwest Research Institute, San Antonio, Texas, USA

Key Points:
- The structure of magnetopause reconnection is determined with ion distribution observations
- Streaming and gyrating ions are discriminated in the reconnected field line region
- The large extension of the reconnected field line region toward the magnetosheath

Correspondence to:
T. Nagai,
nagai@geo.titech.ac.jp

Citation:
Nagai, T., et al. (2016), Thick escaping magnetospheric ion layer in magnetopause reconnection with MMS observations, *Geophys. Res. Lett.*, *43*, 6028–6035, doi:10.1002/2016GL069085.

Received 13 APR 2016
Accepted 18 MAY 2016
Accepted article online 22 MAY 2016
Published online 28 JUN 2016

Abstract The structure of asymmetric magnetopause reconnection is explored with multiple point and high-time-resolution ion velocity distribution observations from the Magnetospheric Multiscale mission. On 9 September 2015, reconnection took place at the magnetopause, which separated the magnetosheath and the magnetosphere with a density ratio of 25:2. The magnetic field intensity was rather constant, even higher in the asymptotic magnetosheath. The reconnected field line region had a width of approximately 540 km. In this region, streaming and gyrating ions are discriminated. The large extension of the reconnected field line region toward the magnetosheath can be identified where a thick layer of escaping magnetospheric ions was formed. The scale of the magnetosheath side of the reconnected field line region relative to the scale of its magnetospheric side was 4.5:1.

1. Introduction

Magnetic reconnection at the Earth's subsolar magnetopause can be classified as asymmetric reconnection due to the large density difference between the magnetosheath and magnetosphere sides (see, e.g., recent reviews by *Fuselier and Lewis* [2011] and *Paschmann et al.* [2013]). The magnetic field intensity is usually small on the magnetosheathside. It is well known that magnetospheric ions flow out through reconnected open field lines into the magnetosheath [e.g., *Cowley*, 1982; *Gosling et al.*, 1990; *Fuselier et al.*, 1991]. The presence of streaming magnetospheric ions on the magnetosheath side of the boundary implies that these field lines are connected to the magnetosphere; however, another magnetospheric ion population can exist. Magnetospheric ions making partial Larmor motion can be observable even in the magnetosheath proper. This can be called the finite Larmor radius effect [e.g., *Wang et al.*, 2014].

In the magnetosphere, high-energy ions usually have isotropic bi-directional distributions (parallel and antiparallel to the field line). In the case where the magnetopause is a simple particle boundary (the tangential discontinuity), magnetospheric ions making partial Larmor motion (red and blue arrows) are observed, as presented in Figure 1a. These ions do not produce any field-aligned flows. In the case of magnetopause reconnection, different characteristics would be observed. When the interplanetary magnetic field (IMF) B_z is southward, magnetospheric ions northward of the reconnection site and magnetosheathward of the shear layer flow out in the antiparallel direction along reconnected field lines. Furthermore, magnetospheric ions making partial Larmor motion can be observed streaming antiparallel to the field rather than bi-directionally (as presented in Figure 1b). This is a very simplified picture. The magnetosphere can supply ions making partial Larmor motion.

Since the magnetic field in the magnetosheath is highly variable and its intensity is fairly weak, in comparison to the adjacent magnetospheric magnetic field, it is usually difficult to distinguish one population from the other. In the case when the magnetosheath magnetic field is steady, these two populations can be discriminated in 3-D velocity distribution functions, and the outer boundary of the reconnected field line region can be identified.

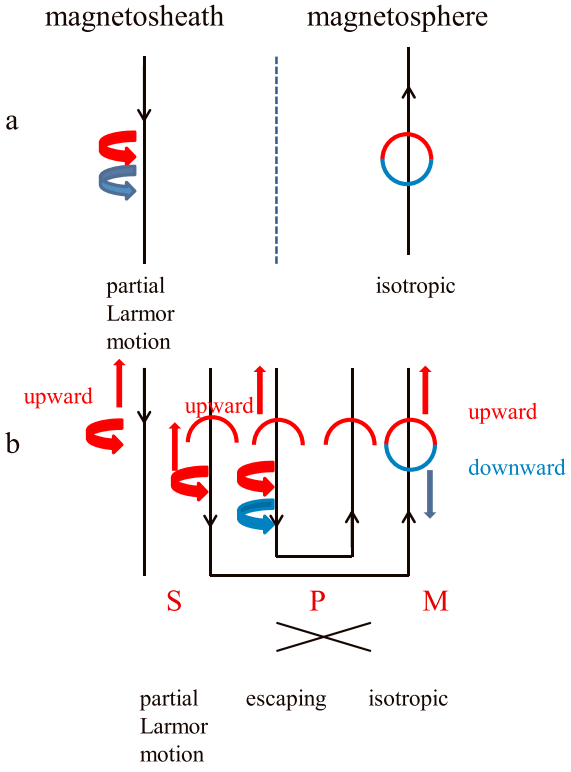

Figure 1. (a) A simple particle boundary (tangentially discontinuous) magnetopause case. Isotropic energetic ions are populated only inside the magnetosphere. Energetic magnetospheric ions making partial Larmor motion can be observed in the magnetosheath. (b) A magnetopause reconnection case (rotational discontinuity). Positions S, P, and M are the magnetosheathside edge of the reconnected field line region, the particle boundary, and the magnetospheric side edge of the reconnected field line region, respectively. Northward of the reconnection site (the X line at the bottom), there is an upward flowing energetic ion layer between S and M. Energetic magnetospheric ions making partial Larmor motion move upward outside S. Energetic ions from the magnetosphere proper can be observed as energetic ions making partial Larmor motion between S and P.

The Magnetospheric Multiscale (MMS) mission consists of four spacecraft and provides high-time-resolution (0.15 s) ion velocity distributions [*Burch et al.*, 2016]. In the early stage of the MMS mission, the interspacecraft separation was beyond 100 km, such that the ion-scale structure could be explored. On 9 September 2015, MMS encountered an ongoing magnetic reconnection at the dusk-side magnetopause during a period of prolonged strongly southward IMF B_z. During this magnetopause encounter, the magnetic field intensity was rather constant across the magnetopause region and the magnetic field intensity was even higher in the asymptotic magnetosheath, leading to robust ion velocity distribution functions being observed at the four spacecraft positions. Because each of the spacecraft observed the boundary layer, its motion could be derived with multispacecraft timing. In this paper, we examine ion distributions in magnetopause reconnection and compare them to the expected ion distributions in Figure 1b in order to determine the relative location of the spacecraft. By timing the crossing of various boundaries, we also determine the spatial scales of the reconnected field line region of asymmetric reconnection at the magnetopause.

2. Overview of the 9 September 2015 Event

On 9 September 2015, the OMNI solar wind data showed that the IMF B_z was almost −10 nT for nearly an entire day and IMF B_y was approximately −5 nT during the period examined. Figure 2 shows the positions of the four MMS spacecraft for the period of 12:37:10–12:38:10 UT in geocentric solar magnetospheric (GSM) coordinates. The center of the spacecraft constellation was located at +4.47 R_E, +8.82 R_E, and −5.52 R_E in GSM, and the radial distance was 9.88 R_E. MMS1 and MMS3 were almost in the same *x-y* plane, and their separation was approximately 120 km. As described later, reconnection outflows were northward, meaning that the spacecraft were located north of the reconnection site (the X line).

Figure 3 shows the magnetic field data (Figures 3a–3d) and ion density data (Figure 3e) from the four spacecraft, and the electron and ion data from MMS3 (Figures 3f and 3g) for the period of 12:37:04–12:38:30 UT. The magnetic field data with 128 Hz sampling are obtained with the fluxgate magnetometer (FGM) [*Russell et al.*, 2016] and are presented in the *LMN* coordinate system, which was determined with Minimum Variance Analysis. The unit vectors obtained from this data interval are $L = (0.1462, 0.7647, 0.6276)$, $M = (0.6506, -0.5523, 0.5213)$, and $N = (0.7452, 0.3322, -0.5782)$ in GSM. The normal direction of the magnetopause (the *N* direction) at each spacecraft position is presented in Figure 2. The magnetic field strength was 40 nT on the magnetosheath side (at 12:37:30 UT) and 30 nT on the magnetospheric side (near 12:38 UT). The ion density, obtained by the First Plasma Instrument (FPI) [*Pollock et al.*, 2016], was approximately 25 cm^{-3} in the magnetosheath and 2 cm^{-3} in the magnetosphere. Since the observed ion and electron densities do not differ significantly, consideration of the effect of cold magnetospheric ions is not needed.

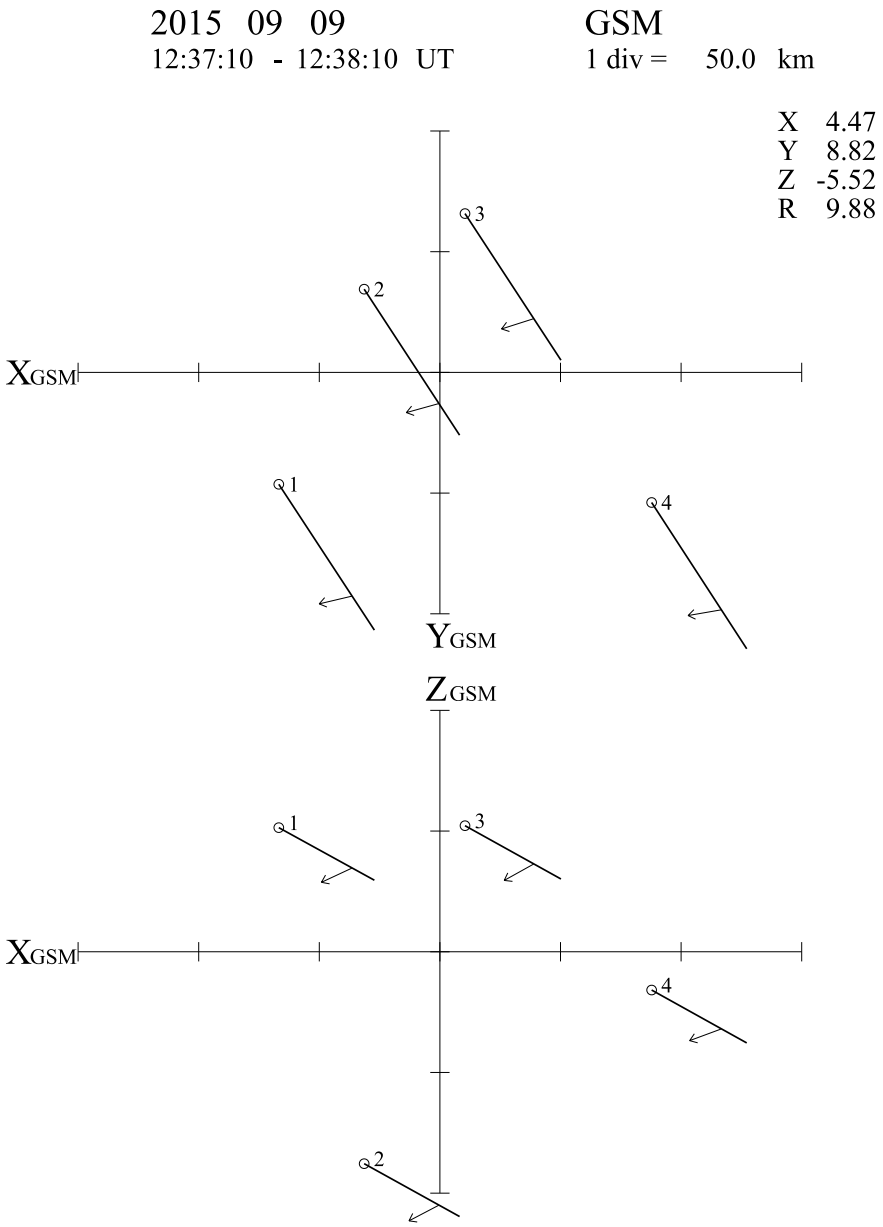

Figure 2. The orbits of MMS1, MMS2, MMS3, and MMS4 in the GSM *x-y* plane (a) and the GSM *x-z* plane (b) for the period from 12:37:10–12:38:10 UT on 9 September 2015. Each circle indicates the position of each spacecraft at 12:37:10 UT. Arrows indicate the magnetopause normal directions.

Until approximately 12:37:39 UT, MMS3 only observed magnetosheath electrons with energies of less than 400 eV, as indicated in the electron energy-time diagram (Figure 3f). The ion energy-time diagram (Figure 3g) shows that there were only magnetosheath ions with energies of less than 5 keV prior to 12:37 UT. Ions (30 keV) first appeared near 12:37:10 UT, and then lower energy ions were subsequently observed until 12:37:40 UT. As discussed in section 3, these keV ions show a half circle pattern in velocity distributions in the $V_{\perp}$ (the velocity perpendicular to the magnetic field) plane, which indicates that these ions were observed as a result of their finite Larmor radii (see Figure 1).

3. Velocity Distribution Functions

In order to determine the characteristics of the reconnected field line region, we examine ion velocity distributions during the reconnection region crossing. The 3-D velocity distribution functions can be obtained

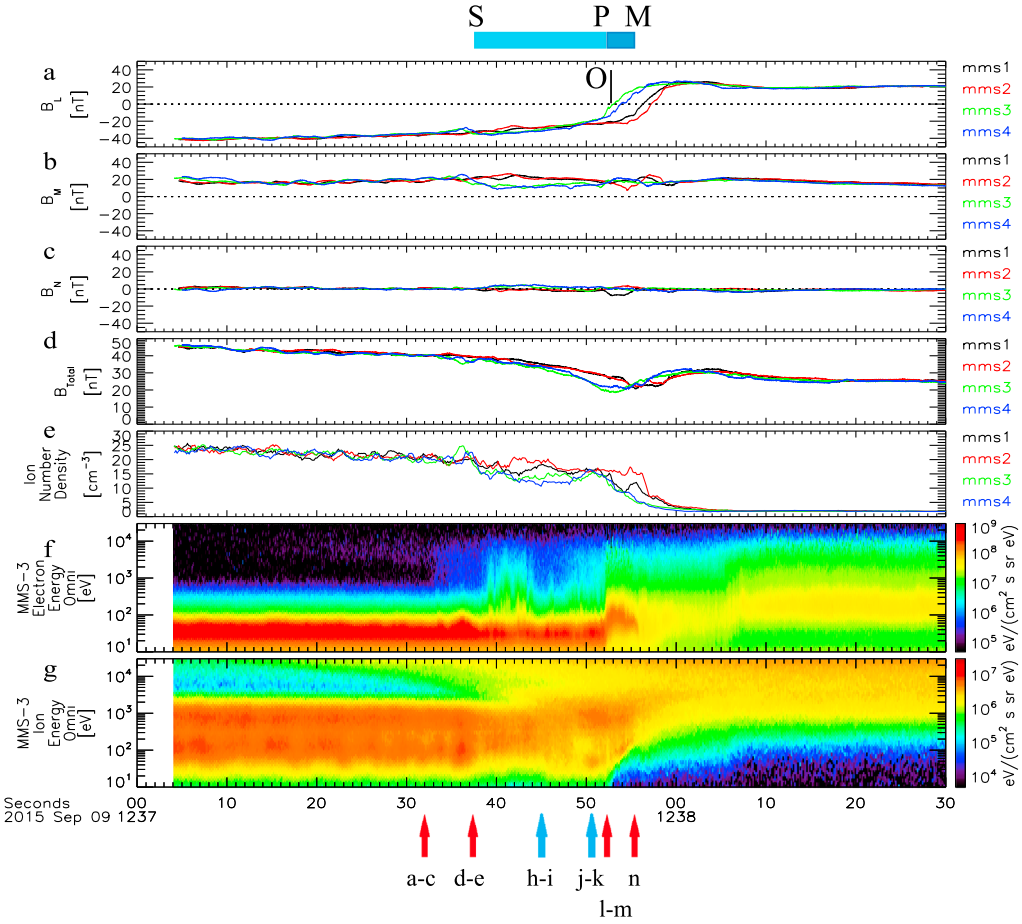

Figure 3. (a–d) The magnetic field data for MMS1, MMS2, MMS3, and MMS4 in the LMN coordinate system for the period from 12:37:04–12:38:30 UT on 9 September 2015. (e) Ion density. (f) Electron energy-time diagram for MMS3. (g) Ion energy-time diagram for MMS3. Arrows labeled a–n at the bottom denote the times at which MMS 3 ion distribution functions a–n (Figure 4) were taken. Positions S, P, M, and O at the top are the boundaries determined from MMS3.

with a time resolution of 0.15 s for the four spacecraft [*Pollock et al.*, 2016]. Although this data set has been examined, we present averaged 3-D velocity distribution functions over 0.9 s for improving count statistics in the $V_{//}$-$V_{\perp 1}$ -$V_{\perp 2}$ coordinate system. Here the $V_{//}$ direction is along the local magnetic field direction, $V_{\perp 1}$ is the direction of the ion flow velocity perpendicular to the local magnetic field, and $V_{\perp 2}$ completes the right-hand coordinate system. The ion velocity moment value is used as the ion flow velocity. In the magnetosheath, $V_{\perp 1}$ is close to the sheath flow direction. Since 5 keV ions (or 1000 km s^{-1} protons) do not originate in the magnetosheath, we present perpendicular cuts of the distribution function ($V_{\perp}$ cuts, hereafter) taken at $V_{//} = +1000$, 0, and -1000 km s^{-1} with velocity range of ±100 km s^{-1}. $V_{//}$ cuts are presented in the $V_{//}$ -$V_{\perp 1}$ plane (within angles of ±20°).

Figure 4 shows representative examples of ion velocity distributions observed by MMS3 and MMS1 during the 9 September 2015 crossing of the magnetopause reconnection region. Figures 4a–4c show $V_{\perp}$ cuts from MMS3 at 12:37:31.9946 UT, which, as mentioned previously, are taken at $V_{//} = +1000$, 0, and -1000 km s^{-1}. Since magnetosheath ions have energies of <5 keV, they are only visible as the central core population in the $V_{\perp}$ cut taken at $V_{//} = 0$ km s^{-1} (Figure 4b). The partial ring distributions, visible in the region of $V > 1000$ km s^{-1} (Figures 4a–4c), indicate that magnetospheric ions with energies >5 keV were undergoing partial Larmor motion. Hence, the spacecraft was inside the magnetosheath proper during the time of this observation (see Figure 1b). It is important to note that more gyrating ions are seen streaming in the antiparallel direction (Figure 4c) than are seen streaming in the parallel direction (Figure 4a). This is consistent with the spacecraft being adjacent to the outflow region and northward of the X line (see Figure 1b and discussion

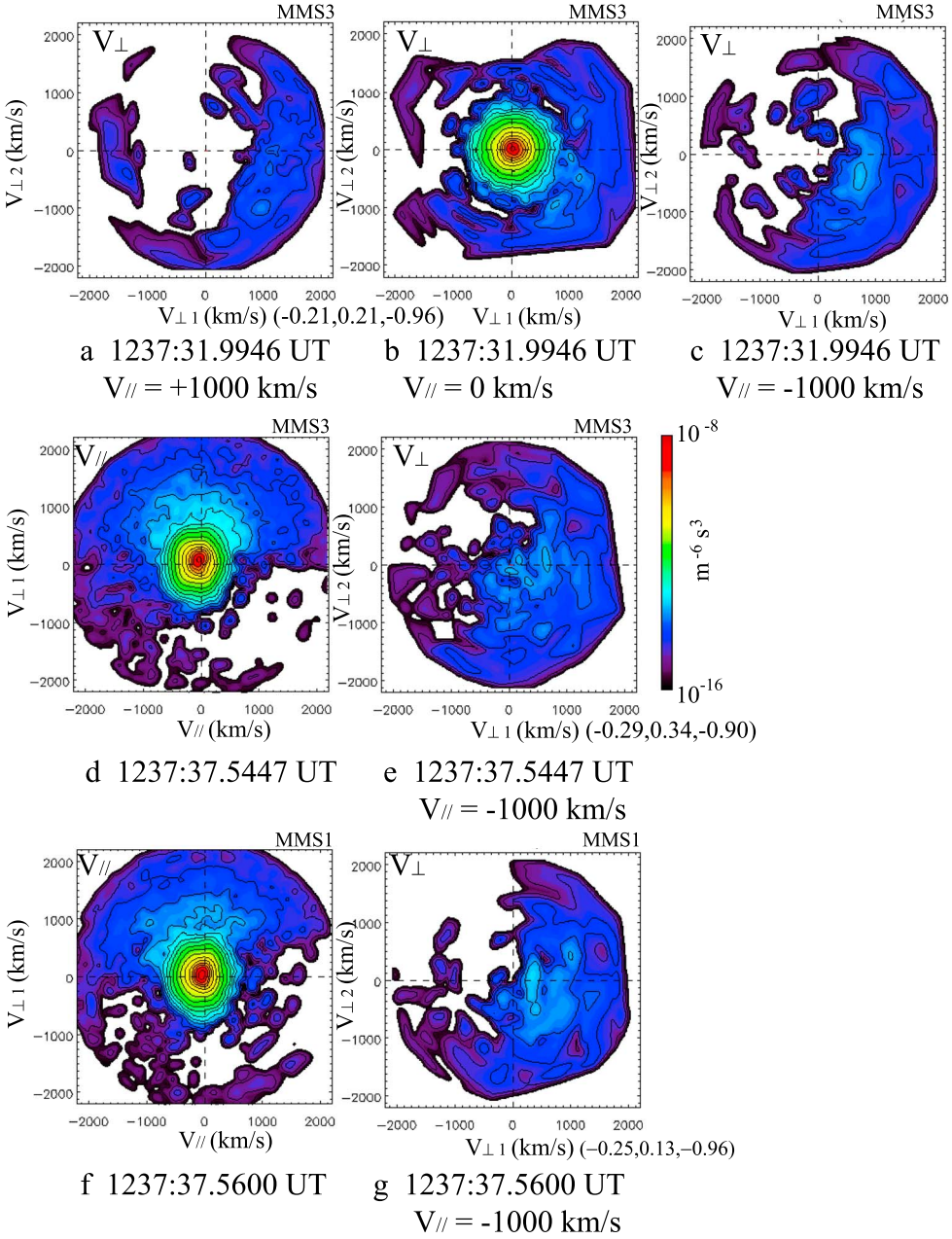

Figure 4. Representative ion distributions from MMS3 and MMS1, which have been averaged over 0.9 s and are shown in the $V_{//}$-$V_{\perp 1}$-$V_{\perp 2}$ coordinates (see text for details). The $V_{\perp 1}$ direction is presented in GSM. (a–c) MMS3 distributions at 12:37:31.9946 UT, (d and e) at 12:37:37.5447 UT, (h and i) at 12:37:44.5941 UT, (j and k) at 12:37:50.7448 UT, (l and m) at 12:37:52.2448 UT, and (n) at 12:37:55.5448 UT. (f and g) MMS1 distributions at 12:37:37.5600 UT. Ion velocity distributions are color-coded according to color bar of logarithm scale, which ranges from 10^{-16} to 10^{-8} m^{-6} s^3. White regions correspond to zero counts.

in section 1). Since the magnetic field B_z is southward ($B_L < 0$) in the magnetosheath, and the reconnection outflow is directed northward, magnetospheric ions with >5 keV are flowing out (in the antiparallel direction) along reconnected field lines.

Figures 4d and 4e show ion velocity distributions from MMS3 at 12:37: 37.5447 UT. A large void area is seen in the $V_{//}$ cut (Figure 4d) for $V_{//} > 0$ and $V_{\perp 1} < 0$ (e.g., the fourth quadrant), which is further indication that the magnetospheric ions entered this observation point as a result of the finite Larmor radius effect (Figure 1b). In the $V_{\perp}$ cut at $V_{//} = -1000\ km\ s^{-1}$ (Figure 4e), ions are observed near the origin ($V_{\perp 1} = V_{\perp 2} = 0$), indicating that 5 keV

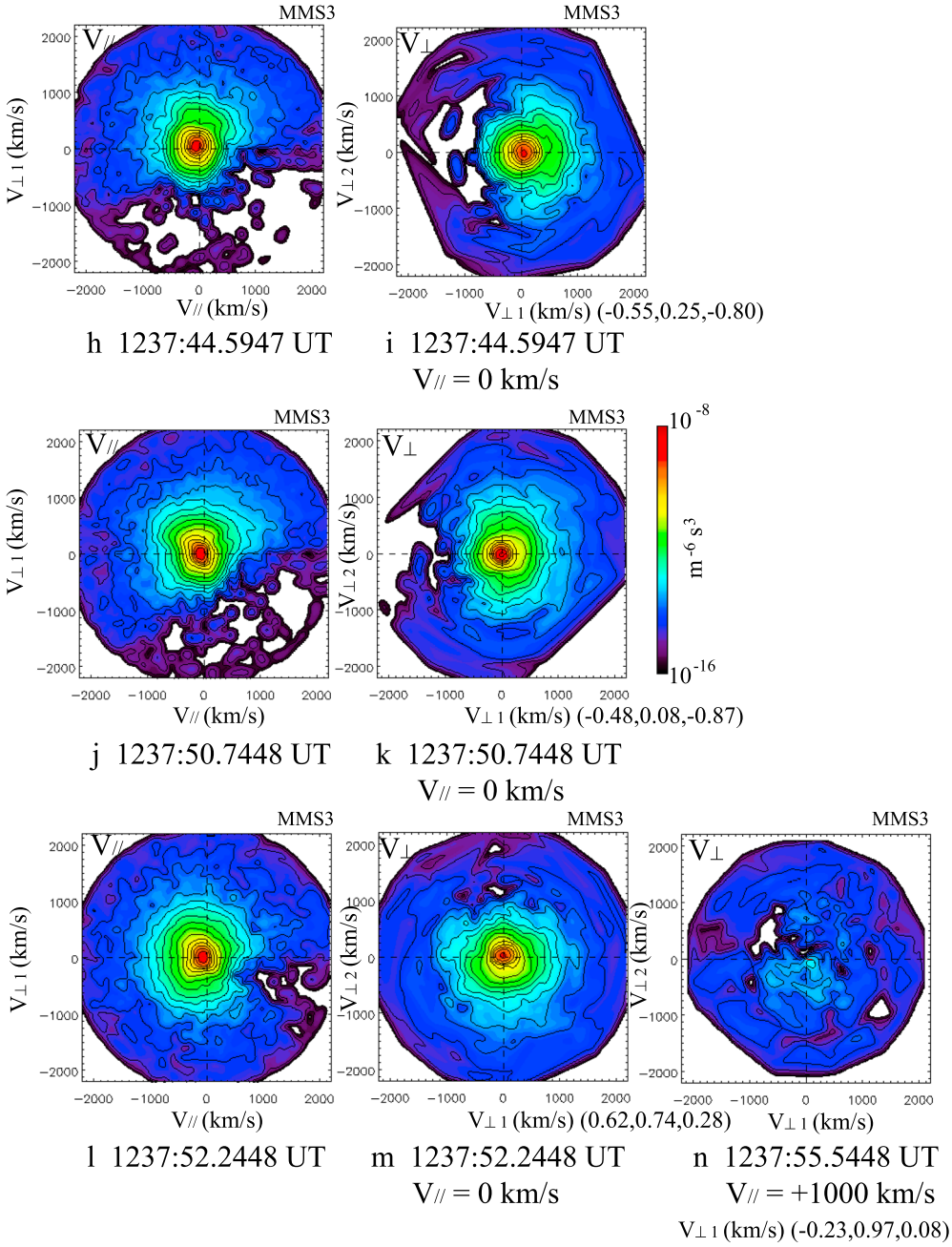

Figure 4. (continued)

magnetospheric ions were streaming northward along the southward field lines ($B_L < 0$). Thus, the spacecraft was located in the reconnected field line region. Hence, the outer boundary of the ion outflow region (position S of Figure 1b) can be identified by field-aligned flows in the $V_\perp$ cut. Figures 4f and 4g show ion velocity distributions from MMS1, which was 120 km apart from MMS3, at 12:37:37.5600 UT (almost the same time as the MMS3 observation). In the $V_\perp$ cut at $V_{//} = -1000\ \mathrm{km\ s^{-1}}$ (Figure 4g), the area around zero is not populated by ions, indicating that there were no 5 keV magnetospheric ions streaming along the field lines ($B_L < 0$) at the MMS1 position. Furthermore, the void area in the $V_{//}$ cut for MMS1 (Figure 4f) is larger than that for MMS3 (Figure 4d). Thus, MMS1 was not yet located inside the reconnected field line region.

Figures 4h and 4i show ion velocity distributions from MMS3 at 12:37: 44.5947 UT. The observed pattern in the $V_{//}$ cut (Figure 4h) is quite similar to that in the previous $V_{//}$ cut (Figure 4d), indicating that MMS3 was still

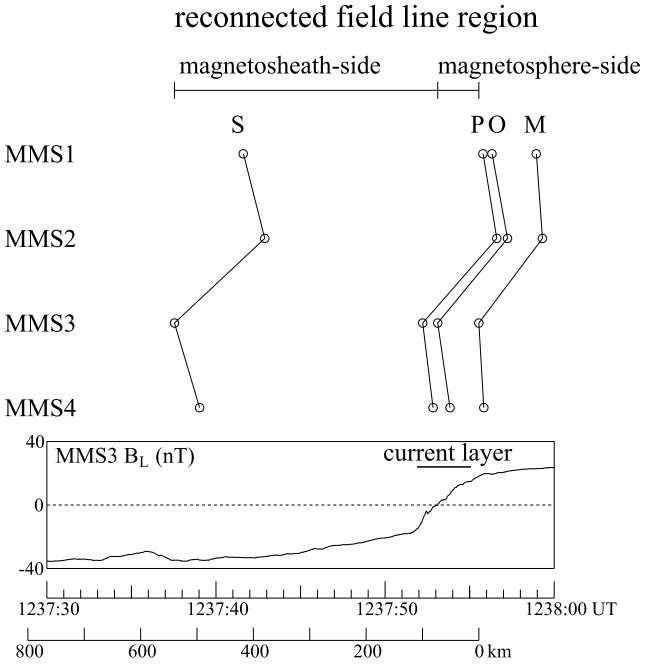

Figure 5. Summary of four spacecraft observations for the magnetopause reconnection region. A time interval of 1 s corresponds to a distance of 30 km. S indicates the magnetosheath side boundary of the reconnected field line region. P indicates the particle boundary between the magnetosheathside and the magnetospheric side of the reconnected field line region. O indicates the field reversal. M indicates the magnetospheric side boundary of the reconnected field line region. The magnetic field B_L data at MMS3 and the current layer interval are also presented.

in the same reconnected field line region. Figure 4i shows that the core ion population has significantly expanded in the positive $V_{//}$ direction, as compared to the core ion population in the magnetosheath proper (see Figure 4b). The expansion further developed prior to the encounter with the field reversal region (at 12:37:53.1122 UT for MMS3), as seen in Figure 4k (12:37:50.7448 UT). As seen in Figures 4d, 4h, and 4j, energetic ions systematically became less anisotropic as the spacecraft approached the field reversal.

Figures 4l and 4m show ion velocity distributions from MMS3 at 12:37:52.2448 UT, when B_L was still negative (i.e., prior to the field reversal). Although ions are still anisotropic in the area of $V_{//} < 0$ in the $V_{//}$ cut (Figure 4l), ions with energies >5 keV become almost isotropic, as seen in the $V_\perp$ cut for $V_{//} = 0\,\mathrm{km\,s^{-1}}$ (Figure 4m). The ion distribution in the $V_\perp$ cut for $V_{//} = +1000\,\mathrm{km\,s^{-1}}$ becomes isotropic at 12:37:55.5448 UT (Figure 4n) when B_L is positive (i.e., following the field reversal). At this time following the field reversal, ions become almost isotropic over the whole energy range.

4. Structure of the Asymmetric Magnetopause Reconnection

The reconnected field line region can be characterized by matching the properties of the ion distributions described in the previous section with the expected characteristics of the ion distributions shown in Figure 1b. The magnetosheathside edge of the reconnected field line region, which is denoted as S in Figure 1b, is identified by the first encounter with parallel streaming energetic ions, which occurred at 12:37:37.5447 (Figures 4d and 4e). The magnetospheric side edge of the reconnected field line region, which is denoted as M, is identified by the first observations of an isotropic distribution function, which occurred at 12:37:55.5448 UT (Figure 4n), since similar isotropic ions observed at later times were of magnetospheric origin. As determined from ion distribution functions, ions with $V_{//} < 0$ first became isotropic at 12:37:52.2448 UT, indicating that this is a particle boundary between the magnetospheric side and the magnetosheathside (denoted as P in Figure 1b). The particle boundary P is located just on the magnetosheath side of the field reversal. The positions S, P, and M can be determined in a similar manner at the other three spacecraft positions, as presented in Figure 5. Here O denotes the field reversal position at each spacecraft.

The density variations in the magnetopause reconnection region (Figure 3e) can be interpreted in the context of these region definitions. The magnetosheath had a number density of 25 $\mathrm{cm^{-3}}$ until 12:37:38 UT. The density decreased to 15 $\mathrm{cm^{-3}}$ near S, then remained relatively constant until the spacecraft crossed the particle boundary P. Inflowing magnetosheath ions were also observed until position P, so that the density did not decrease significantly. The density rapidly decreased in the magnetospheric side of the reconnected field line region, and the density decreased to nearly the asymptotic magnetospheric density near M.

Having defined the timing of spacecraft encounters with these boundary layers, we can determine the spatial scales of the reconnected field line region assuming the constant magnetopause speed of 30 $\mathrm{km\,s^{-1}}$

(determined by the timing method). The reconnected field line region itself has a total width of 540 km. The magnetosheathside of the reconnected field line region has a width of 440 km, and its magnetospheric side has a width of 100 km. Similar asymmetric structures have been reported with multipoint observations of magnetic field line angles by Cluster [e.g., *Lee et al.*, 2014]. These asymmetric structures can be seen far downstream of the X line (the outflow region) for quasi-steady state simulations of asymmetric reconnection [e.g., *Nakamura and Scholer*, 2000; *Tanaka et al.*, 2008; *Pritchett*, 2008]. In the simulation of *Tanaka et al.* [2008], while the density is asymmetrical (the density is higher on the magnetosheath side), the magnetic field intensity is symmetrical. The asymmetry in the reconnection region structure is probably caused by the density asymmetry [see also *Lee et al.*, 2014]. Since the B_L values change from −15 to +15 nT within 3–4 s at the four spacecraft positions, the width of the current layer is approximately 100 km. The bulk of the current is located in the magnetospheric side of the reconnected field line region. This is consistent with the current being carried predominantly by ions inflowing from the high-density magnetosheath in the simulations.

Deformation of the magnetosheath core population can be seen in the region between S and P. The deformation becomes more pronounced as the spacecraft approaches the current layer, as seen in Figures 4i and 4k. The ion energy-time diagram (Figure 3g) shows that all magnetosheath ions are heated inside the current layer. The heated ions in the current layer are probably observed just outside the current layer due to the finite Larmor radius effect. At the duskside magnetopause, the magnetopause is almost parallel to the magnetosheath flow $V = (-40, +60, 0\ \mathrm{km\ s^{-1}})$ direction in GSM and a velocity vector of the farside Larmor motion is toward the $V_{\perp 1}$ direction. This is consistent with the patterns in Figures 4i and 4j.

Outside S, there are two ion populations, one being magnetospheric ions making partial Larmor motion and the other being magnetosheath ions. Ions (30 keV) with pitch angle of 90° are found at ~12:37:12 UT at MMS3 and MMS4, a few seconds later at MMS1, and then at ~12:37:15 UT at MMS2, although it is difficult to determine timings unambiguously.

5. Conclusions

Using multipoint and high-time-resolution ion velocity distributions from MMS during an interval of steady IMF, the structure of the asymmetric magnetopause reconnection region is determined. On 9 September 2015, reconnection took place at the magnetopause, which separated the magnetosheath and the magnetosphere with a large density ratio of 25:2. The magnetic field strength was almost constant across the boundary, although the magnetic field intensity was larger in the asymptotic magnetosheath. The reconnected field line region has a width of 540 km, and the current layer itself has a width of 100 km. The large extension of the reconnected field line region toward the magnetosheath can be identified. The scale of the magnetosheathside of the reconnected field line region relative to the scale of its magnetospheric side is 4.5:1. This field line structure is consistent with the observed density variation.

Acknowledgments
The OMNI solar wind data are obtained in the CDAWeb. The MMS data are available at https://lasp.colorado.edu/mms/sdc/public/. The MMS data are the FPI burst-mode data v2.1.0, and FGM data v4.18.0. We acknowledge Eric Grimes and the developing team of the SPEDAS software for the use.

References

Burch, J. L., T. E. Moore, R. B. Torbert, and B. L. Giles (2016), Magnetospheric multiscale overview and science objectives, *Space Sci. Rev.*, *199*, 5–21, doi:10.1007/s11214-015-0164-9.

Cowley, S. W. H. (1982), The causes of convection in the Earth's magnetosphere: A review of developments during the IMS, *Rev. Geophys.*, *20*, 531–565, doi:10.1029/RG020i003p00531.

Fuselier, S. A., and W. S. Lewis (2011), Properties of near-Earth magnetic reconnection from in-situ observations, *Space Sci. Rev.*, *160*, 95–121.

Fuselier, S. A., D. M. Klumpar, and E. G. Shelley (1991), Ion reflection and transmission during reconnection at the Earth's subsolar magnetopause, *Geophys. Res. Lett.*, *18*, 139–142, doi:10.1029/90GL02676.

Gosling, J. T., M. F. Thomsen, S. J. Bame, T. G. Onsager, and C. T. Russell (1990), The electron edge of the low latitude boundary layer during acceleration flow events, *Geophys. Res. Lett.*, *17*, 1833–1836, doi:10.1029/GL017i011p01833.

Lee, S. H., H. Zhang, Q.-G. Zong, A. Otto, D. G. Sibeck, Y. Wang, K.-H. Glassmeier, P. W. Daly, and H. Rème (2014), Plasma and energetic particle behaviors during asymmetric magnetic reconnection at the magnetopause, *J. Geophys. Res. Space Physics*, *119*, 1658–1672, doi:10.1002/2013JA019168.

Nakamura, M., and M. Scholer (2000), Structure of the magnetopause reconnection layer and of flux transfer events: Ion kinetic effects, *J. Geophys. Res.*, *105*, 23,179–23,191, doi:10.1029/2000JA900101.

Paschmann, G., M. Øieroset, and T. Phan (2013), In-situ observations of reconnection in space, *Space Sci. Rev.*, *178*, 385–417, doi:10.1007/s11214-012-9957-2.

Pollock, C. J., et al. (2016), Fast Plasma Investigation for magnetospheric multiscale, *Space Sci. Rev.*, *199*, 331–406, doi:10.1007/s11214-016-0245-4.

Pritchett, P. L. (2008), Collisionless magnetic reconnection in an asymmetric current sheet, *J. Geophys. Res.*, *113*, A06210, doi:10.1029/2007JA012930.

Russell, C. T., et al. (2016), The magnetospheric multiscale magnetometers, *Space Sci. Rev.*, *199*, 189–256, doi:10.1007/s11214-014-0057-3.

Tanaka, K. G., et al. (2008), Effects on magnetic reconnection of a density asymmetry across the current sheet, *Ann. Geophys.*, *26*, 2471–2483.

Wang, S., L. M. Kistler, C. G. Mouikis, Y. Liu, and K. J. Genestreti (2014), Hot magnetospheric O+ and cold ion behavior in magnetopause reconnection: Cluster observations, *J. Geophys. Res. Space Physics*, *119*, 9601–9623, doi:10.1002/2014JA020402.